

# Toward an Understanding of the High Enantioselectivity in the Osmium-Catalyzed Asymmetric Dihydroxylation. 2. A Qualitative Molecular Mechanics Approach

Per-Ola Norrby,<sup>1</sup> Hartmuth C. Kolb,<sup>2</sup> and K. Barry Sharpless\*

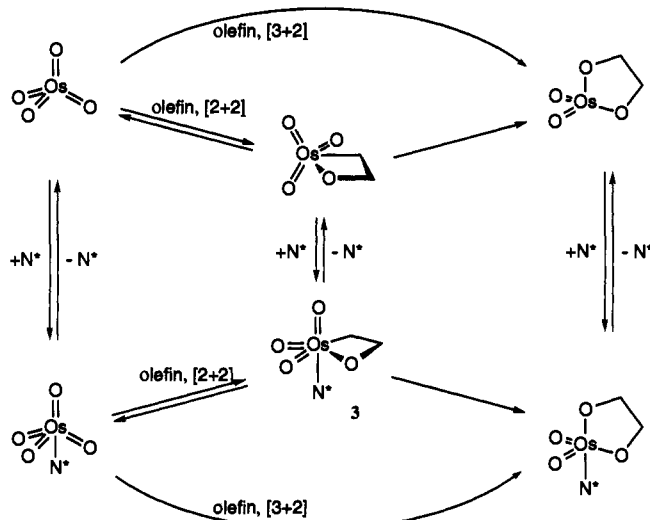
Contribution from the Department of Chemistry, The Scripps Research Institute, 10666 N. Torrey Pines Road, La Jolla, California 92037

Received November 12, 1993. Revised Manuscript Received May 24, 1994\*

**Abstract:** A molecular mechanics (MM2\*) model for the osmium-catalyzed asymmetric dihydroxylation (AD) based on an osmaoxetane intermediate is presented. The high enantioselectivities in the reaction can be rationalized in terms of stabilizing, attractive interactions between the largest oxetane substituent and the O9 substituent on the ligand in addition to repulsive interactions between certain hydrogen atoms in the ligand and the oxetane. The model has been developed to identify the key factors responsible for the observed enantiofacial selectivities as well as to qualitatively explain the selectivity trends observed for the various olefin classes (i.e. mono-, 1,1-di-, *trans*-1,2-di-, *cis*-1,2-di-, and trisubstituted olefins). Stabilizing attractive interactions are considered to be responsible for the much higher enantioselectivities and rate constants observed with the phthalazine ligands in comparison to the first generation ligands, especially with aromatic olefins as substrates.

During the last few years, the osmium-catalyzed asymmetric dihydroxylation (AD) has evolved into one of the most general enantioselective processes known.<sup>3</sup> Several mechanistic proposals have been advanced for this reaction, most of them variations on two basic themes: a concerted [3 + 2] cycloaddition<sup>4</sup> and a stepwise process involving a [2 + 2]-like insertion with subsequent rearrangement.<sup>5</sup> In the AD reaction specifically (not necessarily in all amine accelerated osmium dihydroxylations), we have shown that the rate determining step includes exactly one each of the three principal components: alkaloid ligand, osmium tetroxide, and olefin.<sup>6</sup> We also have shown that the reaction mechanism has to involve at least two sets of diastereomeric transition states.<sup>7</sup> This latter observation is particularly significant, for it would appear to rule out most simple, concerted [3 + 2] mechanistic pathways and thereby provide support for the stepwise [2 + 2]

**Scheme 1.** Some Possible Pathways for the AD Reaction.<sup>3,4</sup> N\* is a Cinchona Alkaloid Derivative



mechanism, since it is the only other mechanism proposed. Using molecular mechanics calculations on a crucial intermediate found by quantum chemical (DFT) calculations,<sup>8</sup> we show here that most currently known features of the AD reaction can be explained in terms of the [2 + 2]-like pathway which involves osmaoxetane intermediates.

## Background

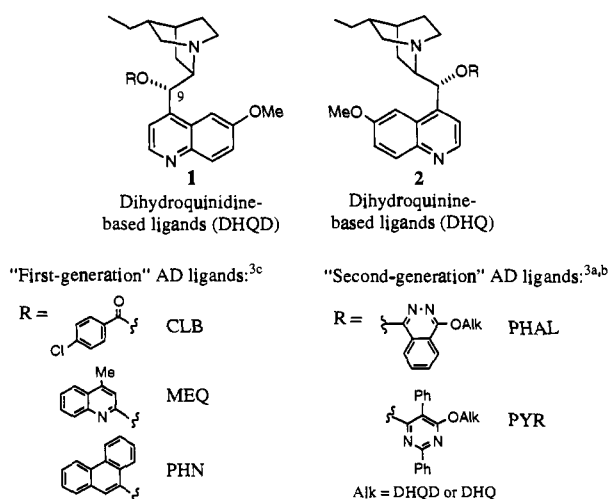
The classical mechanism for the osmylation of olefins is a concerted [3 + 2] cycloaddition mechanism.<sup>4</sup> Accordingly, the rate law of the reaction has been found to be first order in both osmium tetroxide and olefin.<sup>5,9</sup> However, a similar dependence would also be expected for the alternative [2 + 2]-like mechanism.<sup>9b</sup> Certain amine ligands (e.g. pyridine and quinuclidine derivatives) are known to catalyze the reaction, and the cinchona alkaloid-derived ligands **1** and **2** have proven to be especially

\* Abstract published in *Advance ACS Abstracts*, August 15, 1994.  
 (1) Current address: Department of Medicinal Chemistry, Royal Danish School of Pharmacy, Universitetsparken 2, DK-2100 Copenhagen.  
 (2) Current address: Ciba-Geigy Ltd., Central Research Laboratories, CH-4002 Basel, Switzerland.  
 (3) (a) Sharpless, K. B.; Amberg, W.; Bennani, Y. L.; Crispino, G. A.; Hartung, J.; Jeong, K.-S.; Kwong, H.-L.; Morikawa, K.; Wang, Z.-M.; Xu, D.; Zhang, X.-L. *J. Org. Chem.* **1992**, *57*, 2768 and references cited therein. (b) Crispino, G. A.; Jeong, K.-S.; Kolb, H. C.; Wang, Z.-M.; Xu, D.; Sharpless, K. B. *J. Org. Chem.* **1993**, *58*, 3785. (c) Sharpless, K. B.; Amberg, W.; Beller, M.; Chen, H.; Hartung, J.; Kawanami, Y.; Lübken, D.; Manoury, E.; Ogino, Y.; Shibata, T.; Ukita, T. *J. Org. Chem.* **1991**, *56*, 4585. For a review, see: (d) Johnson, R. A.; Sharpless, K. B. *Catalytic Asymmetric Dihydroxylation in Catalytic Asymmetric Synthesis*; Ojima, I., Ed.; VCH: Weinheim, 1993; pp 227-272.  
 (4) (a) Böseken, J. *Rec. Trav. Chim.* **1922**, *41*, 199. (b) Criegee, R. *Justus Liebig Ann. Chem.* **1936**, *522*, 75. (c) Criegee, R. *Angew. Chem.* **1937**, *50*, 153. (d) Criegee, R. *Angew. Chem.* **1938**, *51*, 519. (e) Criegee, R.; Marchand, B.; Wannowias, H. *Justus Liebig Ann. Chem.* **1942**, *550*, 99. (f) Jørgensen, K. A.; Hoffmann, R. *J. Am. Chem. Soc.* **1986**, *108*, 1867. (g) Corey, E. J.; Noe, M. C.; Sarshar, S. *J. Am. Chem. Soc.* **1993**, *115*, 3828.  
 (5) (a) Sharpless, K. B.; Teranishi, A. Y.; Bäckvall, J.-E. *J. Am. Chem. Soc.* **1977**, *99*, 3120. (b) Tomioka, K.; Nakajima, M.; Iitaka, Y.; Koga, K. *Tetrahedron Lett.* **1988**, *29*, 573. (c) Tomioka, K.; Nakajima, M.; Koga, K. *Tetrahedron Lett.* **1990**, *31*, 1741. (d) Jørgensen, K. A.; Schiøtt, B. *Chem. Rev.* **1990**, *90*, 1483-1506. [2 + 2] cycloaddition reactions to form metallacyclobutane complexes can be very fast and reversible; for a review, see: (e) Feldman, J.; Schrock, R. R. *Prog. Inorg. Chem.* **1991**, *39*, 1. Recently, a chromaioxetane was synthesized and characterized, see: (f) Sundermeyer, J.; Weber, K.; Pritzkow, H. *Angew. Chem., Int. Ed. Engl.* **1993**, *32*, 731.  
 (6) Kolb, H. C.; Andersson, P. G.; Bennani, Y. L.; Crispino, G. A.; Jeong, K.-S.; Kwong, H.-L.; Sharpless, K. B. *J. Am. Chem. Soc.* **1993**, *115*, 12226.  
 (7) Göbel, T.; Sharpless, K. B. *Angew. Chem., Int. Ed. Engl.* **1993**, *32*, 1329. The same nonlinear temperature behavior has recently been observed in chemoselectivity studies: McGrath, D. V.; Makita, A.; Sharpless, K. B., manuscript in preparation.

(8) Norrby, P.-O.; Kolb, H. C.; Sharpless, K. B. *Organometallics* **1994**, *13*, 344.

(9) (a) Jacobsen, E. N.; Marko, I.; France, M. B.; Svendsen, J. S.; Sharpless, K. B. *J. Am. Chem. Soc.* **1989**, *111*, 737. (b) Kwong, H.-L. Ph.D. Thesis, Massachusetts Institute of Technology, 1993.

effective in this role. While an osmium glycolate dimer is the end product in the absence of ligand, an osmium glycolate monoligand complex is the normal product if quinuclidine-based ligands are present<sup>10</sup> (Scheme 1). Since the ligand addition to OsO<sub>4</sub> is fast and reversible,<sup>11</sup> the resulting overall reaction is first order in olefin and OsO<sub>4</sub> but shows saturation kinetics for the ligand.<sup>6,9</sup>



Although the [3 + 2] mechanism is consistent with these kinetic observations for the AD reaction, an alternative [2 + 2]-like pathway which is kinetically indistinguishable from the [3 + 2] mechanism is also feasible<sup>9b</sup> (Scheme 1). This latter mechanism invokes a stepwise process involving the formation of an intermediate metallaosetane which then rearranges to the observed primary product, a cyclic osmate ester.

Recent high level quantum chemical calculations by us<sup>8</sup> and others<sup>12</sup> indicate that a complex of type 3 is a plausible intermediate in the AD reaction. A mechanism involving complex 3 is consistent with the observation that the AD reaction proceeds via at least two different pairs of diastereomeric transition states, as deduced from the temperature dependence of the observed enantioselectivity.<sup>7</sup> In contrast, a single concerted [3 + 2] transition state is not compatible with the observed temperature-selectivity behavior. The results indicate that the diastereoselectivities in both transition states are very similar, since the enantioselectivities both below and above the inversion temperature are very similar. The observed temperature dependence of the selectivity could conceivably be a result of a switch from one [3 + 2] pathway to another (i.e. a switch between two alternative pathways in which one involves an axial and an equatorial oxo while the other involves only equatorial oxo's) at the inversion temperature, but it is improbable that two such geometrically different paths would give rise to such similar selectivities. It seems much more reasonable to explain the observations by a switch in the selectivity determining step between two structurally similar transition states flanking the intermediate 3. These results prompted us to attempt rationalizing the features of the reaction by modeling the central osmaoxetane intermediate 3. We invoke the Hammond postulate and propose that this intermediate, having a relatively high energy,<sup>8</sup> should be similar in structure to both of the transition states on the reaction path. In a *qualitative* sense, it may then be possible to rationalize selectivities in the reaction, irrespective of which transition state is determining for the selectivity. To

(10) An alternative pathway has been reported to be second order in ligand, yielding osmate esters with two coordinated ligands as the end product, in the presence of ammonia or pyridine, see: (a) Burton, K. *Biochem. J.* **1967**, *104*, 686. (b) Subbaraman, L. R.; Subbaraman, J.; Behrman, E. J. *Bioinorg. Chem.* **1971**, *1*, 35. (c) Subbaraman, L. R.; Subbaraman, J.; Behrman, E. J. *Inorg. Chem.* **1972**, *11*, 2621. (d) Clark, R. L.; Behrman, E. J. *Inorg. Chem.* **1972**, *14*, 1425.

(11) Kolb, H. C.; Sharpless, K. B., unpublished NMR results.

(12) Veldkamp, A.; Frenking, G. *J. Am. Chem. Soc.* **1994**, *116*, 4937.

this end, we have created a tentative MM2\* force field based upon previously performed quantum chemical (DFT) calculations.<sup>8</sup>

An MM2 model for the osmium dihydroxylation based on an assumed [3 + 2] transition state has previously been published by Houk et al.<sup>13</sup> With this force field it is possible to rationalize the face selectivities obtained in stoichiometric dihydroxylations promoted by chiral diamines. Further work by Houk's group has shown that good predictions can also be obtained for the catalytic AD reactions involving cinchona alkaloid ligands.<sup>14</sup> However, it still remains to be seen if a [3 + 2] model can be found that takes into account the observed nonlinear temperature dependence,<sup>7</sup> one with two [3 + 2] transition states with similar free energies of activation at the inversion temperature, but with a sufficiently large difference in the enthalpy (and entropy) of activation to give an observable break in the enantioselectivity versus temperature curve. Most important, the enantioselectivities for these two hypothetical [3 + 2] paths must be very similar at the inversion temperature.

### MM2\* Parameterization

In the creation of a high quality force field, the parameterization should be based upon as large a range of relevant data as possible. Unfortunately, the postulated intermediate 3 has proved to be very elusive, and it has not been possible to obtain any experimental structural data.<sup>15</sup> A search of the Cambridge Crystallographic database revealed very few polyoxoosmium(VIII) species. The most closely related observable compounds are amine complexes of osmium tetroxide, for which both X-ray and IR data are available.<sup>16</sup> Structural data are also available for the products from osmium dihydroxylations, osmium(VI) glycolates.<sup>17</sup> We have recently shown that density functional theory (DFT) calculations on hypothetical model complexes with ruthenium as the central atom yield structures that correspond closely to the corresponding osmium complexes.<sup>8</sup> In the few cases where polyoxo ruthenium compounds have been structurally characterized, they are very similar to the corresponding osmium structures.<sup>16a</sup> It was also shown that a complex of type 3 was of low enough energy to be a plausible intermediate in the dihydroxylation reaction. It should also be noted here that ruthenium tetroxide has been shown to dihydroxylate olefins in the manner of osmium tetroxide, catalyzed by the same ligands and yielding the same preferred enantiomer.<sup>18</sup>

In the published DFT calculations,<sup>8</sup> ammonia was used as a model for more complex ligands. Ammonia is known to accelerate osmium dihydroxylation,<sup>10a</sup> but in most cases the amines used to effect asymmetric dihydroxylation, and in particular the cinchona alkaloids used in the AD reaction, are tertiary amines. We have, therefore, also optimized structures of type 3 with trimethylamine as ligand and have also investigated the effect of adding a methyl substituent to the two pseudoequatorial positions on the oxetane ring. In these calculations, the oxo groups and the oxetane moiety were almost unaffected by the changes in ligand and ring substituents. The dative nitrogen-metal bond was very long and weak in the optimized structures (>2.9 Å)<sup>19</sup> and is expected to be the most difficult bond to describe quantum mechanically in

(13) Wu, Y.-D.; Wang, Y.; Houk, K. N. *J. Org. Chem.* **1992**, *57*, 1362.

(14) Houk, K. N.; Niwayama, S., private communication.

(15) We have not been able to observe an osmaoxetane intermediate in a photochemically induced osmylation reaction using matrix isolation techniques: McGrath, D. V.; Brabson, G. D.; Andrews, L.; Sharpless, K. B., unpublished results.

(16) (a) Nugent, W. A.; Mayer, J. M. *Metal-Ligand Multiple Bonds*, Wiley: New York, 1988. (b) Svendsen, J. S.; Markó, I.; Jacobsen, E. N.; Rao, C. P.; Bott, S.; Sharpless, K. B. *J. Org. Chem.* **1989**, *54*, 2263. Further X-ray structures obtained in our group were used in the preliminary work: Kolb, H. C.; McGrath, D. V.; Sharpless, K. B., unpublished data.

(17) Pearlstein, R. M.; Blackburn, B. K.; Davis, W. M.; Sharpless, K. B. *Angew. Chem., Int. Ed. Engl.* **1990**, *29*, 639.

(18) (a) Sharpless, K. B.; Akashi, K. *J. Am. Chem. Soc.* **1976**, *98*, 1986. (b) Xu, D.; Sharpless, K. B. Unpublished results.

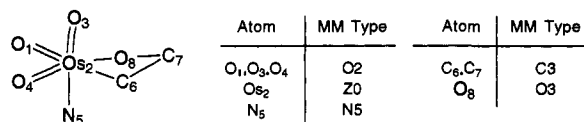


**Figure 1.** MacroModel<sup>22</sup> substructure used in the parameterization with numbering and MacroModel type for each atom.

this type of structure. It was, therefore, shortened to 2.6 Å in the molecular mechanics model to fit more closely the experimentally observed distances in osmium(VIII) complexes, as well as the DFT calculations with ammonia as ligand.

The force field was first parameterized to reproduce as closely as possible the DFT-calculated structure of **3** with trimethylamine as ligand, with and without ring substituents. Several parameters were thereafter varied in order to fit known enantioselectivities, which are the best experimental data available for determination of relative energies in these systems.

It should be stressed that the scarcity of data makes quantitative predictions from these models unreliable. The purpose of this paper is to *qualitatively* identify the factors responsible for the observed face selectivities and rates in the AD reaction. It should also be realized that interactions in the transition states leading to and from this intermediate may differ slightly from those in the intermediate, thereby precluding *quantitative* predictions. However, the strength of our model is that it allows qualitative conclusions about the factors influencing the reaction.

### The Force Field

The van der Waals parameters for the osmium atom were kindly supplied by N. L. Allinger.<sup>20</sup> The values used are  $r^* = 2.31$  Å,  $\epsilon = 0.691$  kcal/mol. Existing MM2\* parameters involving ammonium-type nitrogens were replaced with more recent parameters from the MM2(91) force field,<sup>21</sup> and the C–N dipole was treated as variable in the parameterization. Most of the remaining parameters were implemented for a MacroModel<sup>22</sup> substructure with atom numbering as shown in Figure 1. All new torsional parameters were initially set to zero. The four-membered ring torsionals were given small  $v_3$  components during the refinement in order to reproduce the puckering of the ring. No attempt was made to differentiate between these four values. All stretch–bend interactions involving the metal were set to 0.<sup>23</sup> All parameters involving the Os–N bond as well as the angles between oxetane and oxo groups were regarded as variable in the fit to the experimentally observed enantioselectivities.

The parameters defined for the substructure are given in Table 1 with reference to atoms by substructure number. The remaining parameters are listed in Tables 2–4 with reference by MacroModel<sup>22</sup> atom type. We also added a refined parameter to better describe the bond between the quinoline moiety and the rest of

(19) Constraining this bond to a shorter distance will have very little effect on the calculated energies of optimized structures: Kolb, H. C.; Norrby, P.-O.; Becker, H.; Sharpless, K. B., unpublished data.

(20) Allinger, N. L.; Zhou, X.; Bergsma, J. *Theochem.*, in press.

(21) The parameters used were the ones supplied with MacMimic/MM2-(91) from InStar Software, IDEON Research Park, S-223 70 Lund, Sweden. Many of the parameters were identical. Some were changed: The charge on the N5 atom type was removed. The complexes are neutral, so all charge separations can be handled by dipoles. The special C3(N5)–H1 bond was removed. Changed parameters: N5–C3 no dipole,  $l_0 = 1.499$  Å; C3–N5–C3(–CR<sub>7</sub>)  $\theta_0 = 108.6^\circ$ ; C3–C3–N5–C3  $v_2 = 0.73$ .

(22) MacroModel V3.5X; Mohamadi, F.; Richards, N. G. J.; Guida, W. C.; Liskamp, R.; Caufield, C.; Chang, G.; Hendrickson, T.; Still, W. C. *J. Comput. Chem.* **1990**, *11*, 440.

(23) An investigation of the influence of stretch–bend parameters in the calculation of the vibrational spectrum of osmium tetroxide was performed using MacMimic/MM3(92). With a stretch–bend constant of 0, least-squares optimization of all bending and stretching parameters led to an rms deviation of 19.3 cm<sup>-1</sup> from the experimental spectrum. Reoptimizing with a variable stretch–bend parameter led to an rms deviation of 19.0 cm<sup>-1</sup> (for the very high value of 0.6 for the stretch–bend constant) which shows that the stretch–bend interaction is unimportant in this system.

**Table 1.** Substructure Parameters

parameter type	atoms	$k^a$	$r_0^b$
angle	1–2–3	0.7	116.3
angle	1–2–6	0.2	150.0
angle	1–2–8	0.4	83.72
angle	3–2–4	0.7	113.5
angle	3–2–5	0.15	180.0
angle	3–2–6	0.4	95.5
angle	3–2–8	0.4	101.0
angle	4–2–6	0.4	82.02
angle	4–2–8	0.2	150.0
angle	5–2–6	0.15	75.0
angle	5–2–8	0.15	85.0
angle	6–2–8	0.3	65.0
angle	2–6–7	0.3	96.0
angle	7–6–00 <sup>c</sup>	0.35	117.7
angle	6–7–8	0.4	100.0
angle	2–8–7	0.3	100.0
torsion	3–2–5–00	0.0 <sup>d</sup>	
torsion	8–2–6–7	0.53	
torsion	6–2–8–7	0.53	
torsion	2–6–7–8	0.53	
torsion	6–7–8–2	0.53	

<sup>a</sup> Angle,  $k_b$ , mdyn Å/rad<sup>2</sup>; torsion,  $v_3$ , kcal/mol. <sup>b</sup> Angle,  $\theta_0$ , degrees; torsion, not defined. <sup>c</sup> This value is used for any substituent on C<sub>6</sub>. <sup>d</sup> This value is needed to insure that torsions are not calculated when one angle is 180°.

**Table 2.** Bond Parameters

atom types	$k_s$ (mdyn/Å)	$l_0$ (Å)	bond moment (D)
C3–Z0	4.0	2.21	-0.48
O3–Z0	5.0	2.02	-1.97
O2=Z0	6.7	1.756	-3.53
N5–Z0	0.5	2.60	2.77
C3–N5	5.1	1.499	0.45

**Table 3.** Angle Parameters

atom types	$k_b$ (mdyn Å/rad <sup>2</sup> )	$\theta_0$ (degrees)
O2=Z0=O2	0.7	114.0
O2=Z0–N5	0.14	70.21
00–C3–Z0 <sup>a</sup>	0.35	107.5
Z0–N5–C3	0.21	104.8

<sup>a</sup> The symbol 00 represents any atom. The 00–C3 bond parameter will not be used for angles wholly within the metallaoxetane ring, since the substructure definition (Table 1) overrides this parameter.

**Table 4.** Torsional Parameters

atom types	$v_1$ (kcal/mol)	$v_2$ (kcal/mol)	$v_3$ (kcal/mol)
O3–C3–C2*C2 <sup>a</sup>	0.0	0.83	0.0
00*N5–Z0*00 <sup>b</sup>	0.0	0.0	1.2

<sup>a</sup> This value, defined in a MacroModel substructure, is used only for 4-substituted pyridines.<sup>24</sup> <sup>b</sup> These values are not used with torsions involving the axial oxygen of the complex, since they are already defined in the above substructure (Table 1).

the ligand.<sup>24</sup> Known problems with nonbonded interactions between aromatic rings were alleviated by addition of a 0.7 D dipole to the C2–H1 bond, according to Pettersson and Liljefors.<sup>25</sup>

None of the above values in Tables 1–4 should be considered finalized, but we believe that qualitative conclusions can be drawn from calculations based on this force field.

### Results and Discussion

We have previously shown<sup>3,26</sup> that the stereoselectivity in the AD reaction can be predicted with remarkable success by reference

(24) The torsional parameters for a 4-oxymethylpyridine moiety (in MacroModel O3–C3–C2–C2; in MM2 6–1–2–2) are  $v_1 = 0$ ;  $v_2 = 0.83$  kcal/mol;  $v_3 = 0$ . Wärnmark, K.; Moberg, C.; Akermark, B.; Norrby, P.-O. *J. Comput. Chem.*, in press.

(25) Pettersson, I.; Liljefors, T. *J. Comput. Chem.* **1987**, *8*, 1139.

(26) Kolb, H. C.; Andersson, P. G.; Sharpless, K. B. *J. Am. Chem. Soc.* **1994**, *116*, 1278.

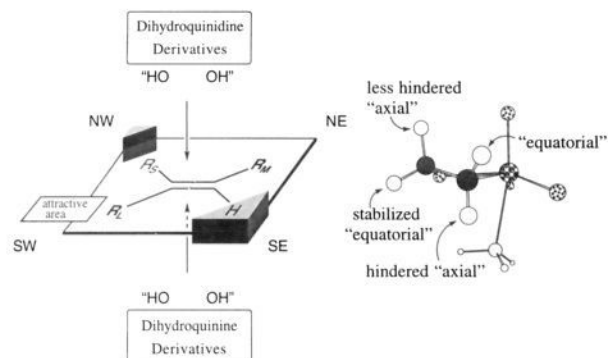


**Figure 2.** Mnemonic device used to predict face selectivity in the AD reaction,<sup>3,26</sup> together with the calculated structure of the intermediate metallaoxetane (**3**).

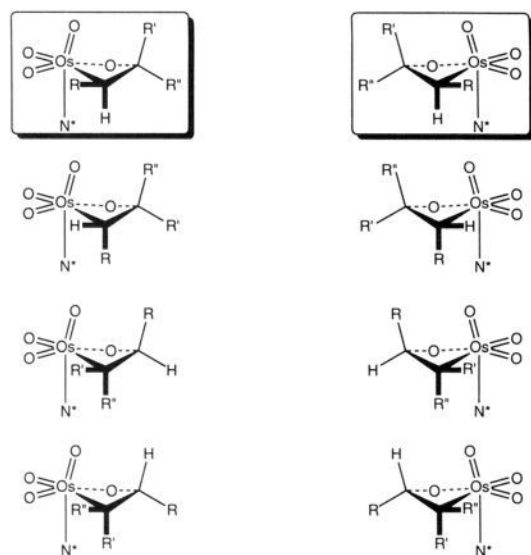


**Figure 3.** Eight possible diastereomers of osmaoxetane intermediate **3** for a trisubstituted olefin reacting in the presence of an enantiomerically pure amine (if the ligand is achiral, then these structures represent four diastereomers and their enantiomers).

to a "mnemonic device" (Figure 2). The substrate is aligned horizontally in the device in such a way as to minimize interactions in the sterically crowded quadrants. The hydroxylation then takes place predominantly either from the  $\alpha$  or  $\beta$  face as determined by the choice of ligand.

Quantum chemical (DFT) calculations<sup>8</sup> on the postulated intermediate (with ruthenium as a model for osmium) indicate that the metallaoxetane ring is puckered and suggest an intriguing correspondence between the four different substituent positions and the four quadrants in the mnemonic device (Figure 2). In the two pseudoaxial positions substituents will experience crowding from other groups on osmium which is most severe in the position pointing toward the amine ligand ("hindered axial" in Figure 2).

With a chiral ligand and a substituted olefin many isomeric forms of the intermediate metallaoxetane **3** are possible. Why then is one form preferred over the others? To illustrate the basis of the high enantioselectivity, we will discuss the different isomeric intermediates **3** in the dihydroxylation of a trisubstituted olefin in the presence of a dihydroquinidine-based ligand. The eight different possible arrangements are shown in Figure 3.

In the case of a trisubstituted olefin six of the eight isomers depicted in Figure 3 can be ignored because any group except hydrogen in the most hindered axial position must lead to severe nonbonded interactions.<sup>27</sup> The remaining two isomers (boxed in Figure 3) are enantiomers in the case of an achiral ligand (e.g. quinuclidine or pyridine). In the presence of a chiral cinchona

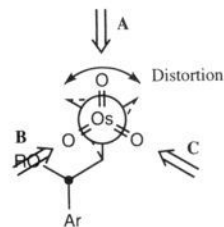


**Figure 4.** Possible modes of constructing the osmaoxetane complexes from the osmium tetraoxide–DHQD–ligand complex. The designations A, B, and C for the equatorial oxygens are chosen to correspond to the direction of formal olefin attack in our previous paper.<sup>26</sup> The ethyl and axial oxo groups are hidden for clarity.

ligand, the boxed structures become diastereomers, but it was not immediately apparent why the difference between these two diastereomers would be large enough to explain the observed enantioselectivity. However, MM2\* calculations on the intermediate in the dihydroxylation of styrene in the presence of dihydroquinidine 4-chlorobenzoate (DHQD-CLB) turned out to be very informative. The X-ray structure of the osmium tetraoxide complex of an AD ligand is available<sup>16b</sup> (Figure 4), and it is similar to the structure calculated for the osmaoxetane complexes. The different isomers of the oxetane complex can be conceptually<sup>28</sup> created from the osmium tetraoxide–cinchona ligand complex by distorting an equatorial oxo group  $\approx 30^\circ$  either clockwise or counterclockwise around the N–Os–O axis and then adding either the *si* or the *re* side of the olefin in a [2 + 2] fashion with the least substituted carbon toward the osmium. This yields four different diastereomeric osmaoxetane intermediates (Figure 3, top row, either R' or R'' is phenyl, the remaining substituents are hydrogen). Notice that if the olefin is trisubstituted or symmetrically *trans*-1,2-disubstituted, only two diastereomers are produced. This is an important point and we will return to it later.

Depending on which oxo group is used for the operation (A, B, or C, Figure 4), three rotameric forms of the four diastereomers are created, yielding a total of 12 main isomers of the intermediate in this reaction (the conformational preferences of the ligand are discussed below). Seven of the most interesting optimized isomers of this intermediate are shown in Figure 5.

We found that one conformation of a diastereomer [(R)-I-rotamer B in Figure 5], leading to the observed major product, indeed had a lower energy than any of the other 11 isomers [the (R)-I-rotamer B isomer is  $>5$  kJ/mol lower in energy than the best *S* isomer, in qualitative agreement with the experimentally observed ee, 71%<sup>29</sup>]. Our calculations reveal that this outcome is a result of a stabilization of the styrene phenyl ring, available only in the B rotameric forms, by beneficial nonbonded (van der Waals and dipole–dipole) interactions with the chlorobenzoate moiety of the ligand. Rappé has previously invoked similar nonbonded interactions to rationalize a fascinating regioselectivity effect in the asymmetric hydroformylation reaction.<sup>30</sup>

(27) The isomers in the third row of Figure 3 could alleviate some of the strain by adopting an inverse puckering, but unless R'' is also hydrogen the conformations would still be of high energy due to interactions with both the amine ligand and osmium. Kinetic and thermodynamic factors should generally favor formation of the metallaoxetane isomer in which the metal is bound to the least substituted olefinic carbon, and in the present study we have made the simplifying assumption that this is the isomer through which the rearrangement to glycolate proceeds. However, given the rapid and reversible metallacycle equilibria believed to precede the rate determining rearrangement to glycolate, the other metallaoxetane isomer (i.e. more substituted olefinic carbon bound to osmium), even if present as a minor component, could also be a glycolate precursor. Evidence that this alternative pathway is of minor importance (at least in the AD process) will be presented in a future publication.

(28) Chemically, the intermediate could be formed in two different ways: by ligand addition to the preformed oxetane or by olefin addition to the ligand–tetraoxide complex (cf. Scheme 1). At the present time, we can not differentiate between these two reaction paths. The formation mode in Figure 4 was chosen because it is easier to visualize.

(29) Kwong, H.-L.; Sorato, C.; Ogino, Y.; Chen, H.; Sharpless, K. B. *Tetrahedron Lett.* **1990**, *31*, 2999.

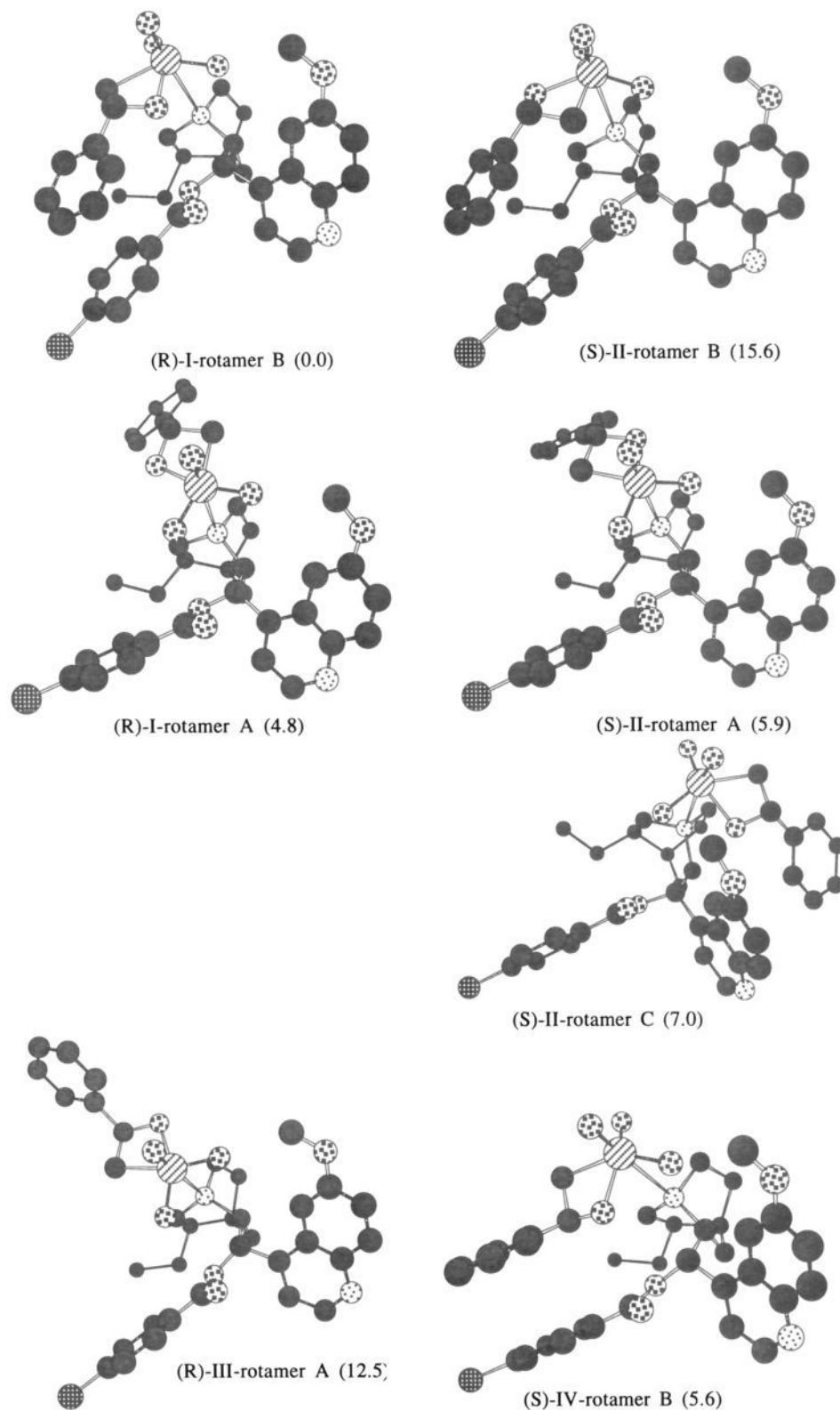


**Figure 5.** Seven intermediates calculated for the dihydroxylation of styrene catalyzed by DHQD-CLB. Being a DHQD derivative, this ligand favors the (*R*)-diol. The hydrogen atoms are hidden for clarity. The four diastereomeric forms are labeled by Roman numerals, their rotameric forms by the letters A, B, and C (cf. Figure 4). Isomers I (two top left) and III (bottom left) have the *R* configuration at the styrene  $\alpha$ -carbon and lead to (*R*)-diol, whereas isomers II (three top right) and isomer IV (bottom right) are progenitors of the (*S*)-diol. Energies (in parentheses) are in kJ/mol relative to the global minimum [(*R*)-I-rotamer B, top left].

The calculation results in our present study correspond well with our kinetic studies<sup>26</sup> where these effects have been experimentally demonstrated. In particular, it was shown that the reaction rate was highest when large aromatic groups, which

can experience strong stacking stabilization, were present in both the ligand and the substrate. The conformational search also yielded noninteracting isomers (rotameric forms A in Figure 5). In the isomers where the olefinic substituent and the AD ligand

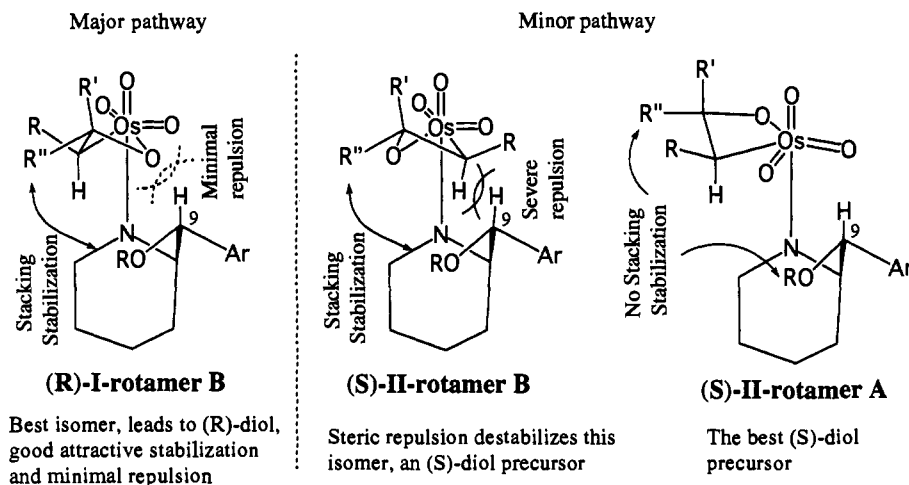


**Figure 6.** Interplay of two crucial interactions, one attractive, the other repulsive, provides a simple rationale for the effectiveness of the AD reaction.

side chain are on opposite sides of the oxetane ring (diastereomers III and IV), inverse puckering of the oxetane ring was found. In rotameric form B, these isomers may experience attractive stabilization from the chlorobenzoate moiety [exemplified by isomer (S)-IV-rotamer B in Figure 5, bottom right] but at the cost of additional crowding between the oxetane and quinuclidine moieties.<sup>31</sup> Nevertheless, as shown by the relative energies, significant amounts of the *S* enantiomer may be formed by this pathway. However, no isomers with this inverted puckering were found in our DFT calculations,<sup>32</sup> so we cannot be sure whether this type of conformation is an artifact or not.

One isomer in Figure 5 [(S)-II-rotamer C] exemplifies the third possible rotameric form around the N–Os bond. It is clear from this and other diastereomers of rotamer C that the quinoline moiety cannot significantly stabilize the intermediate through stacking interactions with the phenyl substituent. Rather, it experiences severe crowding from the metallaoxetane in any isomer where it is close enough to realize such stacking interactions with the phenyl ring. Generally, rotamers of type C are higher in energy than those of type A.<sup>33</sup>

It should be noted that there is a slight difference in energy between the two diastereomers I and II in rotameric form A ( $\approx 1$  kJ/mol, Figure 5, second row). This difference results from a skewing or twisting of the quinuclidine moiety due to repulsions between its large C9 substituent and its bicyclic framework. The degree of twist is most pronounced in the dihydroquinidine (DHQD) ligands where the location of the ethyl substituent works to enhance it. In the dihydroquinine (DHQ) ligands the effect of the ethyl group is to mute the inherent twist imparted by the C9 substituent. In any case, this twisting usually favors the *R* intermediates in any rotameric conformation and may explain why a DHQD-based ligand generally gives slightly higher enantioselectivity than its DHQ-based analog. In cases where severe steric crowding precludes the formation of rotameric form B (and C), this may indeed be the only factor determining enantioselectivity.

The balance between the possible pathways is delicate and quite sensitive to the choice of parameters. A very weak bond between the ligand and the metal center favors the inverse puckering mode (which has not been observed in our DFT calculations), whereas a hard, short bond increases steric repulsion

between the ligand and oxetane moieties and thus disfavors rotamer B. We know that inverse puckering (isomers III and IV) as well as rotameric forms A and C must be of minor importance at least for the styrene case, for the following reasons: inverse puckering favors the (S)-IV diastereomer over (R)-III, whereas only *R* diastereomers lead to the observed major product. The kinetic studies mentioned above<sup>26</sup> show conclusively that the ligand O9 substituent and an olefin substituent interact in a stabilizing way, which is impossible in conformations A and C. We have tried to account for this in the parameterization, but the importance of the inverse puckering, which favors the (S)-IV isomer, may still be overestimated in our current force field. Part of the problem may be the hard hydrogens in MM2, which is known to give too strong repulsions at close distances.<sup>34</sup> With a softer hydrogen, the optimum metal–ligand bond distances for the force field would be shorter, which disfavors the inverse puckering.

To clarify the difference between the diastereomers (R)-I and (S)-II in Figure 5, we will return again to the case of the trisubstituted olefin. The picture is simpler here for only two diastereomers (I and II) need be considered since the lone hydrogen substituent of the olefin must be in the hindered “axial” position (*cf.* Figure 2). The reason for the dissimilarity of the diastereomeric intermediates is illustrated in Figure 6.

In the (R)-I-rotamer B form, the R'' group in the olefin can easily interact favorably with the OR moiety of the ligand. The (S)-II diastereomer, on the other hand, can only experience the same stabilizing stacking interactions in the rotamer where the pseudoaxial hydrogen interferes strongly with the tertiary hydrogen on C9 of the quinuclidine side chain. In order to alleviate this crowding, the (S)-II diastereomer can swing open to adopt rotameric form A which is energetically preferable despite the loss of stabilization possible in the B form. Our experimental studies clearly demonstrate that the size and the nature of the OR group is critical for the reaction with respect to osmium binding, rate, and enantioselectivity.<sup>26</sup> When the OR and the methoxyquinoline groups are both replaced by methyl groups, as in 2-isopropylquinuclidine, the increased steric bulk around the quinuclidine core leads to drastically reduced binding to osmium.<sup>26</sup> In essence, the OR substituent allows good binding but replacing it with a slightly larger CH<sub>3</sub> substituent shuts it down, underscoring the exquisite steric sensitivity in close to the binding site. The oxygen atom and the flat quinoline moiety are just small enough to enable binding to OsO<sub>4</sub>.

In addition, the R group which is attached to the oxygen atom linker at C9 should have a large platelike shape, preferably

(30) Castonguay, L. A.; Rappé, A. K.; Casewit, C. J. *J. Am. Chem. Soc.* **1991**, *113*, 7177.

(31) For the reasons outlined below (*cf.* Figure 5), isomer (S)-IV (in rotameric form B) will have a lower energy than isomer (R)-III.

(32) An unsubstituted ring with inverse puckering will revert to the normal puckering mode during geometry optimization in the DFT calculations.

(33) Naturally, no restrictions were placed on conformational searches, but for the olefins investigated, no dominant form of rotamer C has been found, even in cases where steric crowding disfavors rotamer B.

(34) The hydrogen is believed to be too hard in MM2 and has been adjusted in the more recent MM3: Allinger, N. L.; Yuh, Y. H.; Lii, J.-H. *J. Am. Chem. Soc.* **1989**, *111*, 8551.

aromatic in nature, which is projected under the R'' group (Figure 6) to provide the attractive, stabilizing interactions which are so clearly evident in these reactions.<sup>26</sup> It is noteworthy that the balance between these two (S)-II rotamers (A and B, Figures 5 and 6) is delicate. In certain cases where large aromatic groups furnish enough stabilization, the rate of formation of the S product is also increased (relative to systems where the OR ligand moiety is small), albeit much less than that of the R product.<sup>26</sup> In this case, the attractive forces are large enough to overcome the repulsion between the four-membered ring and the C-9 hydrogen, making rotamer B the preferred conformation for the (S)-II diastereomer. When the stabilizing contribution is weaker, (S)-II-rotamer A becomes the preferred intermediate in the pathway leading to the S enantiomer. Nevertheless, the absence of stabilization in rotamer A still disfavors the S relative to the R product [via (R)-I-rotamer B].

Since the above analysis offers a simple rationale for the enantioselectivity in the AD reaction, its key features are worth reiterating. The two intermediates on the left in Figure 6 (rotameric forms B) are very similar and both partake of the attractive stacking interaction between substituents R'' on the olefin and OR on the ligand. The difference between (R)-I and (S)-II is that the carbon and oxygen atoms connected to osmium in the metallacycle have been interchanged. This simple switch gives rise to a severe H-H repulsion for the (S)-II diastereomer in rotameric form B. If this analysis is correct, then, intriguingly, the AD is crucially dependent on a noncovalent attractive interaction for its high selectivity. The role of the attractive interaction is to favor a transition state arrangement where a repulsive steric effect is a serious problem for one diastereomer [(S)-II], but not for the other [(R)-I]. In this scenario, the AD's enantioselectivity arises from the interplay of two simple effects, attraction and repulsion. Primacy is assigned to the attractive effect, since it ordains the decisive role played by the repulsive interaction.

The importance of the stabilizing stacking interactions involving the equatorial R'' substituent, in addition to the repulsive interactions involving the hindered "axial" group closest to the amine, leads to some interesting corollaries (see Figure 6). A large group can best experience stabilization if it is *cis* to a hydrogen. This affords a good rationalization for the relatively poor performance of most ligands with *cis* olefins. The good results obtained with most trisubstituted and *trans* disubstituted olefins are also in agreement with this model, since these olefins have a hydrogen atom in the appropriate position. The lower enantioselectivities for monosubstituted or *cis*-disubstituted olefins compared to *trans*-disubstituted olefins may be due to the alternative pathway which involves an attack of the olefin from the face leading to the minor enantiomer and with inverse puckering of the ring [isomers (R)-III and (S)-IV]. Such isomers may be formed only from these two classes of olefins (the requirement is that two hydrogens are *cis* to each other), and they will experience crowding from the quinuclidine moiety and in addition, for the B rotamers, some attractive stabilization from the aromatic OR substituent of the ligand. The 1,1-disubstituted olefins can form intermediates of type I, rotamer B, by attack on either face of the olefin. The enantioselectivity here should mainly result from the different attractions the two substituents register for the binding site of the ligand. In addition, this substitution pattern leads to a flattening of the oxetane ring, which disfavors rotamer B due to additional crowding.

Large flat groups which are *cis* to a hydrogen (Figure 6) will also have a favorable influence on the rate of the reaction.<sup>26</sup> It has long been known that the enantioselectivity is best when the olefin substituents are modestly large and/or aromatic, but the dramatic rate increase in the reaction when complementary large flat moieties are present in both the olefin and the ligand is a more recent and very interesting finding in our group.<sup>26</sup>

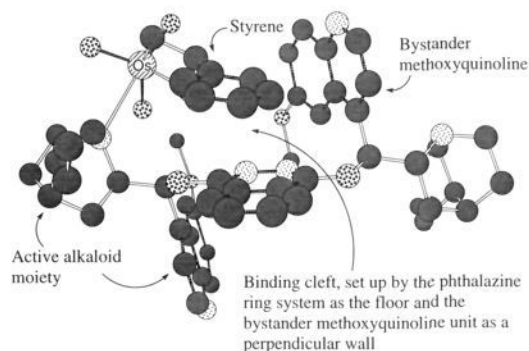
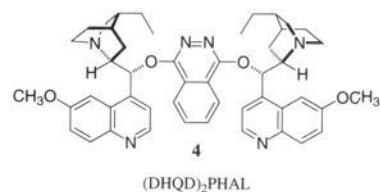


**Figure 7.** Calculated structure for the most important intermediate in the styrene dihydroxylation using (DHQD)<sub>2</sub>PHAL (**4**). This structure corresponds to (R)-I-rotamer B in Figure 6.

The discussion so far has been centered around the first generation of ligands,<sup>3c</sup> where simple esters or ethers of the parent alkaloids were used. A quantum leap was taken in the AD reaction a few years ago with the advent of the "dimeric" ligands based on a heterocyclic spacer, e.g. phthalazine **4**.



Despite the apparent C<sub>2</sub> symmetry of these ligands, we have shown that ligand effectiveness is retained, and in some cases slightly improved, when one of the DHQD moieties is exchanged for certain nonbasic groups.<sup>6</sup> This establishes that only one alkaloid unit is needed in the AD reaction and, we believe, validates the use of the same computational model for these "dimeric" ligands. The global minimum for the putative oxametallacycle intermediate from calculations on the dihydroxylation of styrene with bis(dihydroquinidyl)phthalazine (**4**) is shown in Figure 7.

The most interesting feature of this ligand is that it appears to present a binding cleft with the phthalazine core as the floor and with the bystander methoxyquinoline moiety providing an abutting, perpendicular wall. Figure 7 demonstrates how the phenyl group of the substrate fits snugly into this cleft, experiencing attractive face-to-face and edge-to-face interactions.<sup>35</sup> These interactions are much more efficient than those of the "first generation" ligands,<sup>3c</sup> due to the unique structure of the phthalazine ligand. The enclosing character of this ligand is reminiscent of the active site of some enzymes. One prediction which can be made from this model is that olefin substituents that are too large to fit within the cleft should reduce or even destroy the selectivity, and this in fact has been observed.<sup>36</sup> Groups that are reasonably flat but large will cause the bystander quinoline to be rotated away, in effect converting the ligand to a first generation AD ligand. This effect is also noticeable as a decrease in the reaction rates for these olefins.<sup>36</sup>

(35) Offset parallel interactions between aromatic systems can be attractive and they become more favorable with increasing size of the arene. For a model which explains the geometric requirements for interactions between aromatic systems, see: (a) Hunter, C. A.; Sanders, J. K. M. *J. Am. Chem. Soc.* **1990**, *112*, 5525. See also: (b) Jorgensen, W. L.; Severance, D. L. *J. Am. Chem. Soc.* **1990**, *112*, 4768. (c) Cozzi, F.; Cinquini, M.; Annunziata, R.; Dwyer, T.; Siegel, J. S. *J. Am. Chem. Soc.* **1992**, *114*, 5729. (d) Cozzi, F.; Cinquini, M.; Annunziata, R.; Siegel, J. S. *J. Am. Chem. Soc.* **1993**, *115*, 5330.

(36) Recent investigations show that both the enantioselectivities and rate constants drop on increasing the size of the substituents of 3,5-disubstituted styrenes, probably because large substituents disfavor the stacked arrangement shown in Figure 6; Becker, H.; Ho, P. T.; Kolb, H.; Loren, S.; Norrby, P.-O.; Sharpless, K. B. *Tetrahedron Lett.*, in press.

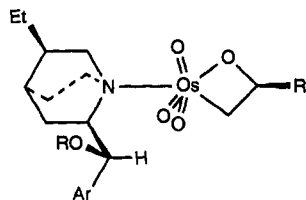


**Figure 8.** Hypothetical intermediate in the AD reaction based on the calculated, high energy isomer of the ligated osmaoxetane.

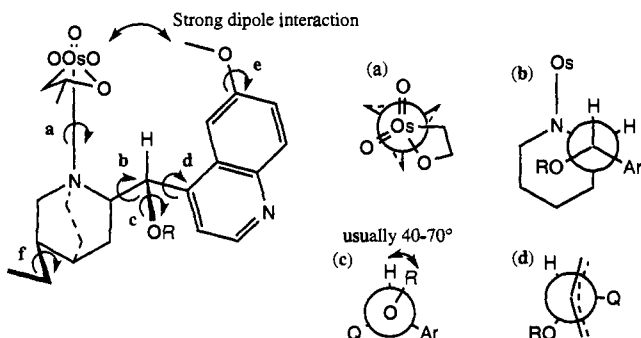


**Figure 9.** Important flexible bonds in the osmaoxetane complex with an AD ligand.

Corey and Noe<sup>37</sup> recently suggested, based on ocular inspection of CPK models of a dimeric macrocyclic ligand similar to **4**, that the selectivity of the process is due to a sandwiching of the olefinic moiety between the two quinoline units. However, molecular mechanics calculations show that their suggested conformation is of relatively high energy, both for the free ligand and its osmium complexes. Interestingly, even in their system a conformation similar to that in Figure 7 has a low energy. Their model also lacks the edge-to-face interactions which are usually more stabilizing than face-to-face interactions.<sup>25,35</sup>

Conceivably, there could be other octahedral isomers of **3** which have the amine ligand positioned trans to the ring carbon or the ring oxygen. In the DFT calculations none of these are minima on the energy hypersurface. Geometry optimization will convert both starting structures to the same distorted trigonal bipyramid, where all oxo's are equatorial and the oxetane ring occupies one apex. This isomer is calculated to be higher in energy than the oxetane **3** which is favored in this work.<sup>8</sup>

Making the reasonable assumption that the olefin will be oriented in such a way that the least substituted carbon is connected to the metal, it can easily be seen that there can be no close proximity between the ligand and the substituent on the olefin (RO and R, Figure 8). Therefore a model based on the high energy isomer would be unable to rationalize the observed kinetic effects in the AD reaction.<sup>26</sup>

### Conformational Analysis

The AD ligands give a first impression of being very flexible. This has prompted us to make extensive conformational searches utilizing the pseudosystematic Monte Carlo search routine in MacroModel.<sup>22</sup> As it turned out, for many different systems and different versions of the force field only a few variations are allowed. The main degrees of freedom are shown in Figure 9 and discussed below.

The possible conformations of the oxetane ring vary with the type of olefin and have been partly discussed above. Here we will concentrate on the ligand part of the complex. In terms of a conformational search, the most important structural element in the complex is the N-Os bond (a). In the Newman projection it can be seen that complete staggering of all substituents is impossible. It is inappropriate, therefore, to assume a normal

3-fold rotation around this bond. Consequently, in the full conformational searches this bond was given an initial resolution of 12, corresponding to a step of 30°. As it turned out, the oxetane ring behaves as though it was only one "averaged" ligand. Rotation around this Os-N bond, followed by minimization, gives rise to the three main rotameric forms types shown previously (Figure 5, A, B, and C, respectively).

Bond b has a normal 3-fold rotation. It can easily be seen in the models that any binding to osmium is impossible unless the C-H bond is approximately parallel to the N-Os bond.<sup>16b</sup> In the AD ligands this positions the relatively small ether or ester linkage (RO-) close to the quinuclidine. It has been shown experimentally<sup>26</sup> that switching the position of the RO group with the more bulky quinoline unit Ar (i.e., epimerizing C-9 in the cinchona alkaloid) strongly disfavors binding to osmium.

The Newman projection of bond c shows the normal preferred conformation of an ester or aromatic ether of a secondary alcohol. In all our searches the R group has ended up between the hydrogen and quinoline substituents with a dihedral angle to the hydrogen of 40–70°. A recent investigation of bond type d (i.e., an oxymethyl pyridine type bond) has shown that the C-O bond actually has a small preference for eclipsing with the pyridine ring.<sup>24</sup> Since neither the C-O bond nor the C-H bond has any strong bias against near eclipsing with the aromatic ring, the bond to the sterically demanding quinuclidine will be almost perpendicular to the quinoline ring. There are two such conformations but only the one shown is of low energy. Rotating the quinoline by 180° gives rise to a high energy minimum with strong steric crowding between the ether/ester unit (RO, Figure 9) and the 5-position in the quinoline ring and no favorable dipole interaction between the quinoline methoxy and the osmium moiety.

The methoxy group will be eclipsed with the aromatic ring (bond e). Rotation by 180° from the conformation shown gives another minimum where much of the dipole interaction (in MacroModel this is actually a charge-charge interaction) is lost, generally resulting in an increase in the steric energy by about 4 kJ/mol. This conformational preference is in accordance with earlier NOE studies.<sup>16,26</sup> Bond f has a normal 3-fold rotation. Different conformations here have little effect upon the relative energies of R and S isomers in the same kind of conformation (Figure 5) but will make small contributions to the relative energies of, for example, rotamers A and B.

### Limitations of the Model

The model as presented here has some limitations that preclude its use as a quantitative prediction tool for the AD reaction. We know from the DFT calculations that the dative nitrogen-metal bond is weak and flexible, and such bonds are difficult to model accurately with the covalent bond model in most molecular mechanics force fields. We are able to obtain especially good results for monosubstituted aromatic olefins. However, for some other olefins with bulky/branched substituents, the system is not flexible enough to accommodate the increased steric bulk in the otherwise stabilized position. With the best known *monomeric* ligands (the phenanthryl ethers (PHN)) for this "poorer fitting" class of olefins, calculations indicate that the aromatic moiety on O9 of the ligand is no longer positioned under the oxetane ring but rather on one side (Figure 10); this causes the oxetane to rotate away and thereby partially disengages the repulsive C9-hydrogen/oxetane-hydrogen interactions (Figure 6) which are crucial to the enantiodifferentiating ability of the system. In part, this may be due to the hard hydrogens in MM2,<sup>34</sup> giving too much steric bulk for the alkyls, but in these specific cases we believe a model based on the transition state of the oxetane rearrangement would yield better results (cf. Figure 10). Here it can be seen that the (R)-I isomer (rotamer B) offers a much more facile rearrangement path compared to the (S)-II isomer, which experiences additional obstruction when rearranging to

(37) Corey, E. J.; Noe, M. C. *J. Am. Chem. Soc.* **1993**, *115*, 12579.



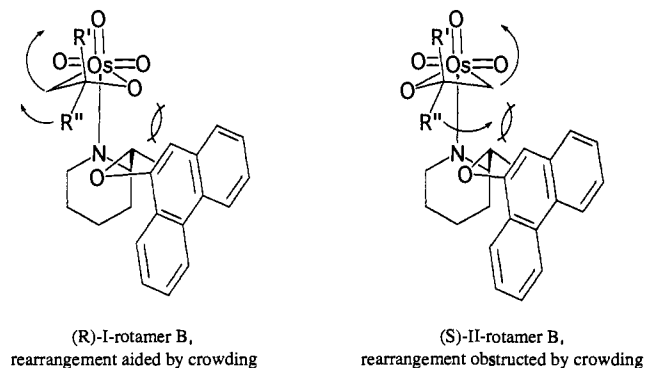


**Figure 10.** Rearrangement modes for the two isomeric intermediates. The  $R''$  group is close in space to the phenanthryl moiety. Vectors for rearrangement to the glycolate are indicated.

the product. Thus, relatively high selectivities may be obtained even if the isomers (R)-I and (S)-II (both in rotameric form B) have similar energies.

The "crowding" effects on the rearrangement are quite general and will increase the energy advantage of the (R)-I path in most systems. It is most pronounced in ligands where the stabilizing group is tilted up on one side of the oxetane or when, as in the phthalazine ligands (PHAL), the bystander part of the ligand forms a "wall" on one side of the stabilizing site. This could be the major factor explaining the fact that our model underestimates the enantioselectivity for the PHAL ligands.

We know from the parameterization work that the energetic difference between the different isomers shown in Figures 5 and 6 is sensitive to the choice of parameters. The lack of input data together with this sensitivity is what makes the model unreliable as a quantitative tool for enantioselectivity predictions. Therefore, the important part of this work is not the force field per se but rather the qualitative conclusions we have been able to draw from it concerning the specific interactions which determine the rate and selectivity in this reaction. The excellent agreement between these conclusions and the observed kinetic data and selectivities makes us confident that we have indeed identified the key selectivity determining features of the AD reaction.

### Summary

We have shown that many features of the osmium-catalyzed asymmetric dihydroxylation (AD), such as ligand acceleration,

stabilizing stacking interactions,<sup>26</sup> the high enantioselectivity, the face selectivity, and the trends for different classes of olefins, can be rationalized by molecular mechanics calculations on the previously postulated intermediate 3. This intermediate is believed to be structurally closely related to the selectivity-determining transition state in the reaction, in accordance with the Hammond postulate. The enantiofacial selectivity is governed chiefly by two factors: stabilizing stacking interactions between the substituents on the olefin and O9 of the ligand and destabilizing repulsive interactions between the oxetane ring and H9 of the ligand. These repulsive interactions selectively destabilize the transition state leading to the minor diastereomer. The excellent results obtained with the dimeric second-generation ligands are attributed to an enzyme-like binding pocket, facilitating both binding and further reaction of one diastereomeric intermediate selectively. The formation and subsequent rearrangement of the intermediate 3 will be further investigated in order to refine the computational model.

### Computational Details

All DFT calculations have been performed on a Cray Y-MP computer using the UniChem DGauss 1.1.1 program.<sup>38</sup> The DZVP basis set supplied with the program has been used for all atoms. The Becke-Perdew nonlocal correction was applied self consistently. Molecular mechanics calculations have been performed using MacroModel V3.5<sup>22</sup> and V4.0 on Iris Indigo machines, with a modified MM2\* force field described in this paper. The osmium environment has been treated as a MacroModel substructure, with differentiation between oxo's in different positions. Conformational searches were performed with the pseudosystematic Monte Carlo search in MacroModel, choosing the number of conformations to search all possible combinations at the selected torsional resolution (usually 500–10000 conformations). Projections of 3D structures have been created with the Chem3D Plus program.<sup>39</sup> Influence of the stretch-bend term was investigated using the MacMimic/MM3(92) package.<sup>21</sup>

**Acknowledgment.** This work has been supported by the National Institutes of Health (GM 28384) and the National Science Foundation (CHE 8903218). P.-O. Norrby thanks the Swedish National Science Research Council and the Foundation Bengt Lundkvists Minne for travel grants. H. C. Kolb thanks the Deutsche Forschungsgemeinschaft for a fellowship. We are grateful to professor T. Liljefors for helpful discussions. We also wish to thank professors G. Frenking and K. N. Houk and Dr. S. Niwayama for disclosure of unpublished material.

(38) DGauss 1.1.1, part of UniChem 1.1.1 from Cray Research, Inc.

(39) Chem3D Plus for Macintosh, Cambridge Scientific Computing Inc., 875 Massachusetts Av., Suite 61, Cambridge, MA 02139.